Available online at www.sciencedirect.com

ScienceDirect

Ceramics International 37 (2011) 1393–1399

CERAMICS
INTERNATIONAL

www.elsevier.com/locate/ceramint

Porous alumina-spinel ceramics for high temperature applications

Rafael Salomão [a,b,*], Mariana O.C. Villas Bôas [a], Victor C. Pandolfelli [a]

[a] *Materials Engineering Department (DEMa), Federal University of São Carlos (UFSCar), Rodovia Washington Luís, km 235, São Carlos, SP, Brazil*
[b] *São Carlos School of Engineering (EESC-SMM), University of São Paulo (USP), Avenida Trabalhador São-Carlense, 400, 13566-590 São Carlos, SP, Brazil*

Received 10 September 2010; received in revised form 11 October 2010; accepted 4 January 2011
Available online 3 February 2011

Abstract

In order to reduce energy costs, high-temperature insulation porous refractory ceramics have been subjected to increasing demands. Among the techniques used to produce these materials (such as the addition of foaming agents and organic compounds), the pore generation via phase transformation presents key aspects, such as easy processing and the absence of toxic volatiles. In this study, this technique was applied to produce porous ceramics by decomposing an aluminum–magnesium hydro-carbonate known as hydrotalcite ($Mg_6Al_2(CO_3)(OH)_{16}\cdot 4H_2O$). It was found out that by using this complex compound, a large fraction of pores can be generated and kept at high temperatures (above 1300 °C) due to the *in situ* formation of spinel-like phases ($MgAl_2O_4$).
© 2011 Elsevier Ltd and Techna Group S.r.l. All rights reserved.

Keywords: Porous ceramics; Phase transformation; Hydrotalcite; Spinelization

---

1. Introduction

High-temperature (>1000 °C) thermal insulating products are fundamental in reducing the energy costs in the cement, steel, aluminum, iron-alloy and petrochemical industries. Among the suitable materials for this purpose, porous ceramics are outstanding because they combine intrinsic ceramic properties, such as chemical inertness and refractoriness, with low thermal conductivity. Besides saving energy, the diminished heat loss to the environment also improves working conditions minimizing the employees' stress as a result of their exposure to high temperatures. In addition to thermal insulating, porous ceramics can be used in many other applications such as filters for hot gases or liquid metals, substrates for chemical and biological catalysts and implants [1,2]. This variety of applications has been motivating in terms of developing various processing methods. Among the most described in the literature, three of them are briefly presented below.

1.1. Decomposition of organic matter

The incorporation of organic compounds induce pore formation after their burnout, when previously mixed with inorganic ones [3–8]. Individual organic particles (such as non-dissolved starch, wood flour or seeds) or a continuous phase (thermoset resins, hot water dissolved starch and sodium alginate, etc.) can be used for this purpose. In some cases, organic particles are previously coated with the inorganic ones and then packed into a mold, after which a ceramic slurry is poured in [4]. It is also possible, by using additives and pH adjustments, to induce opposite charges on the surface of organic and inorganic particles in order to generate an ordered coagulation, known as heterocoagulation [5,8]. In this case, a fraction of smaller pores greater than those obtained by simply mixing these raw materials can be attained. Two important concerns lie in this method: firstly is the generation of toxic volatiles during burnout; secondly, depending on the organic content, hot gas release can damage the surrounding structure [8].

1.2. Foamed porous ceramics

This consists of adding a surfactant to the ceramic slurry, which is vigorously stirred to incorporate air bubbles [9–14]. This technique was subsequently optimized by firstly preparing

---

* Corresponding author. Present address: São Carlos School of Engineering (EESC-SMM), University of São Paulo (USP), Avenida Trabalhador São-Carlense, 400, 13566-590 São Carlos, SP, Brazil. Tel.: +55 16 33738672.

E-mail addresses: rsalomao@sc.usp.br (R. Salomão), vicpando@power.ufscar.br (V.C. Pandolfelli).

0272-8842/$36.00 © 2011 Elsevier Ltd and Techna Group S.r.l. All rights reserved.
doi:10.1016/j.ceramint.2011.01.012

the foam and then adding it to the suspension, allowing for a better control of the diameter and number of pores. The compatibility of electric charges between the surfactant and ceramic particles, the shear rate used and the foam stability are the main variables that directly affect the porous structure by using this approach. More recently, a promising variation of this technique was developed [13,14]. Stabilizing the liquid phase of the foam with ceramic nanoparticles (with a diameter below 100 nm) instead of only organic surfactants, results in a thin closed-packed structure on the surface of the bubbles, which is preserved after freeze-drying and sintering. The great interest in this method is the high porosity and mechanical strength attained.

1.3. Decomposition of hydrated/carbonated inorganic compounds

Similar to the decomposition of organic matter, this technique is based on generating pores through the volume reduction that follows the dehydroxylation or decarbonation reactions [15–17]. Because it does not release toxic volatiles and it uses low cost compounds and raw materials that can be easily incorporated into the ceramic slurries, it can be pointed out as a tough and more practical solution when high temperature insulation is the objective.

The material most commonly used as a pore generator in dense alumina matrixes is aluminum hydroxide ($Al(OH)_3$), which presents a 60 vol.% reduction, when heated above 600 °C [18–20]. By this approach, structures suitable for application such as filtering elements can be attained with porosity in the range of 62–82% [17]. However, when calcined thermally decomposed $Al(OH)_3$ samples are heated above 1100 °C, an unexpected effect can be observed: the Al_2O_3 phase transformations result in highly reactive transition aluminas and sub-micrometric pores that, in contact with the alpha-alumina matrix, favor sintering and lead to porosity reduction of the material [18–20].

In order to overcome this drawback, $Al(OH)_3$ with a smaller surface area can be used, resulting in less reactive particles and samples with larger pores. The relationship between the pore diameter and densification was experimentally shown by processing samples with the same pore-former volume content, but with different particle diameters. It was shown that the finer the particle, the higher the densification of the samples [19,20,22]. However, it was not clear whether this mechanism used to delay the phase transformation, is effective when the ceramics are continuously kept at high temperatures.

In the present work, the hydroxide decomposition method was selected to produce porous ceramics for applications at temperatures close to 1500 °C, using various inorganic compounds in combination with an alumina matrix. For this purpose, the pore inducers (different grades of aluminum hydroxides and hydrotalcite, $Mg_6Al_2CO_3(OH)_{16}\cdot 4H_2O$) were characterized regarding their density and mass loss thermal behavior. For the porous samples attained, apparent porosity and pore size measurements were carried out after firing at 1100 °C, 1300 °C and 1500 °C for 5 h.

2. Materials and methods

All powders used as pore-formers were previously dried at 110 °C during 24 h. After this step, their density and surface area were measured in AccuPyc 1330 helium pycnometer and BET equipment (Micrometrics, USA), respectively. The hydrotalcite was previously prepared as a combination of 50 vol.% of caustic magnesia (Magnesita S.A., Brazil, 94 wt.% MgO, $D_{50} = 100\ \mu m$ and surface area = 20 m^2/g) and 50 vol.% of hydratable alumina (Alphabond 300, Almatis, US, with $D_{50} = 6\ \mu m$, 88% Al_2O_3 and surface area = 165 m^2/g). These raw materials were mixed with 50 wt.% of distilled water (no dispersants were added) and autoclaved at 150 °C for 10 h. After this period, the hydrotalcite was dried at 110 °C for 24 h and ground in a tungsten carbide mill for 30 min.

The testing samples were prepared with various proportions of calcined alumina, calcium aluminate cement (CAC, Secar 71, Kerneos, France), water, a polyethyleneglycol based dispersant (BASF, Germany) and pore-formers, varying: (a) the content of $Al(OH)_3$ (from 30 up to 70 vol.%, using Hydral 9280, Almatis, USA), (b) the $Al(OH)_3$ mean particle size (50 vol.% content) and (c) the hydrotalcite content instead of the $Al(OH)_3$ one (30–97.5 vol.%). Calcined alumina-free (97.5 vol.% hydral 9280 and 2.5 vol.% CAC) reference samples were also tested in the same conditions. Characteristics of the raw materials and of the compositions tested can be found in Table 1.

After mixing for 5 min, the suspensions were cast as 25 mm × 25 mm cylinders and cured in a humid atmosphere, at 50 °C, for 24 h. Afterwards they were dried at 110 °C for 24 h and thermally treated at temperatures ranging from 1100 °C, 1300 °C and 1500 °C, with a heating rate of 2 °C/min for 5 h.

After firing, the porosity of the samples was measured by the immersion method (kerosene oil as immersion fluid, five samples). Their pore size was measured by mercury porosimetry, using a Micrometrics 9320 Porosimeter (the curves presented are mean values from two samples).

Their mechanical strength was measured under diametrical compression, according to the ASTM C496-90 standard, in MTS 810 TestStar II equipment, with a loading rate of 11 N s^{-1}. Five samples were tested for each condition.

The volumetric shrinkage (VS) of the samples was accessed by measuring the samples' dimensions before (BF) and after firing (AF) and using the expression:

$$VS = 100\% \times \frac{\{[(H_{BF}.\pi.(D_{BF})^2/4] - [(H_{AF}.\pi.(D_{AF})^2/4]\}}{[(H_{BF}.\pi.(D_{BF})^2/4]} \tag{1}$$

where H and D are, respectively, the height and diameter of the cylindrical samples. The mean values presented were obtained after testing 5 samples.

These results (porosity, pore size, mechanical strength and volumetric shrinkage) are presented as mean values with the standard deviation error bars.

Table 1
Characteristics of the raw materials and compositions tested.

Characteristics of the raw materials	Matrix		Pore formers			
	Calcined alumina (A1000SG)[a]	Calcium aluminate cement (Secar 71)[b]	Aluminum hydroxide			Hydrotalcite[c]
			Hydral 9280[a]	Hydrogard GP[d]	C30[d]	
Density (g cm^{-3})	3.94	2.97	2.43	2.42	2.42	2.16
Surface area (m^2 g^{-1})	7.45	0.97	3.71	0.72	0.04	12.3
Mean particle diameter (D_{50}, (m)	0.53	25	1.80	13	106	17
Vol.% in the suspensions	67.5, 47.5, 27.5 or 0	2.5	30, 50 or 70, 97.5	50	50	30, 50, 70 or 97.5

Water content	Polyethyleneglycol based dispersant[e]
70 wt.% (based on the weight of the powders)	2–2.5 wt.% (based on the weight of the powders)

[a] Almatis, US.
[b] Kerneos, France.
[c] Previously synthesized.
[d] Alcoa, Brazil.
[e] BASF, Germany.

X-ray diffraction was carried out for the ground material ($D_{Part} < 45$ μm) (XRD, Siemens D 5000, Kristalloflex 710, Kα = Cu, Ni filter) for some of the 1500 °C fired samples.

3. Results and discussion

3.1. Different $Al(OH)_3$ contents

Fig. 1 points out the effects of the $Al(OH)_3$ content on the apparent porosity of the samples. Initially, for those fired at 1100 °C, it can be observed that the greater the $Al(OH)_3$ content, the higher the porosity level attained, as a result of the volume reduction that follows $Al(OH)_3$ decomposition [16–18]. For the high temperature thermal treatments (1300 °C and 1500 °C), lower porosity levels were attained, with minor differences between the different pore former contents. These results suggest that the pores initially formed at 1100 °C were partially eliminated by the sintering/densification processes [19,21].

This behavior can be understood considering the thermal reactions involving $Al(OH)_3$, from its decomposition up to the sintering temperatures. The $Al(OH)_3$ thermal decomposition is carried out in the temperature range of 250–450 °C (depending on the particle size and surface area), as presented by Eq. (2):

$$2Al(OH)_3 \rightarrow Al_2O_3 + 3H_2O \qquad (2)$$

During this process, $Al(OH)_3$ undergoes a volumetric contraction of about 60%, due to the density mismatch between aluminum hydroxide ($\rho_{Al(OH)_3} = 2.42\,g\,cm^{-3}$) and the oxide ($\rho_{Al_2O_3} = 3.98\,g\,cm^{-3}$) [15]. If $Al(OH)_3$ particles are initially added to a calcined alumina matrix, during their decomposition, this contraction generates pores, because up to 1100 °C the matrix does not present any significant volume reduction due to sintering. However, after its decomposition, aluminum hydroxide becomes a highly reactive and surface area defect-rich compound, known as transition alumina. When added to a calcined alumina matrix, transition aluminas can significantly enhance the driving force for sintering and densification at temperatures above 1100 °C. This effect can be pointed out as the main cause for the low porosity values attained for the samples fired above 1100 °C [21] (Fig. 2).

For the 97.5 vol.% $Al(OH)_3$ sample, no suitable mechanical strength to be handled or to perform porosity measurements after thermal treatment was observed. This effect is associated to the combination of excessive pore formation with intense

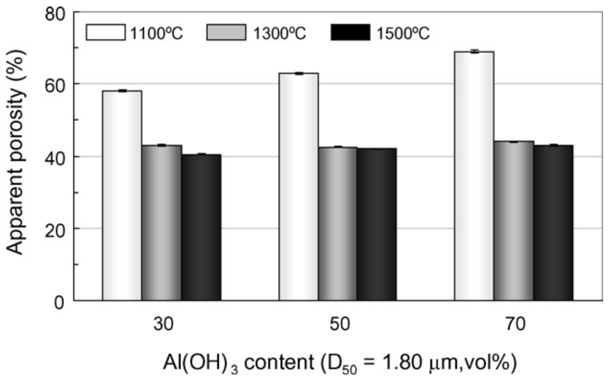

Fig. 1. Apparent porosity of the samples prepared with 30, 50 and 70 vol.% of $Al(OH)_3$ (D_{50} = 1.80 μm), fired at 1100 °C, 1300 °C or 1500 °C for 5 h.

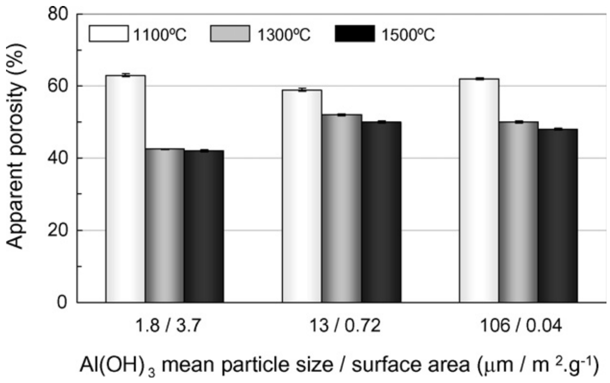

Fig. 2. Apparent porosity for the samples prepared with 50 vol.% of $Al(OH)_3$ with different mean particle size, fired at 1100 °C, 1300 °C or 1500 °C for 5 h.

sintering, generating a thin dense area surrounding large pores [16]. The $Al(OH)_3$-free sample, on the other hand, presented low porosity levels (respectively, 35%, 22% and 20% after firing at 1100 °C, 1300 °C and 1500 °C) because they were only related to the water content initially present in the suspension for casting and to the decomposition of hydrated calcium aluminates and aluminum hydroxide originated during CAC hydration.

3.2. Different $Al(OH)_3$ mean particle sizes

Reports in literature pointed out that increasing the $Al(OH)_3$ mean particle size could lead to lower densification because (i) after decomposition, coarse $Al(OH)_3$ results less reactive alumina and (ii) the large pores generated (Fig. 3) would be greater than the critical value for sintering [22]. In order to evaluated this hypothesis, samples were prepared by the same procedure, but with 50 vol.% of various sources of $Al(OH)_3$, with different average particle size (D_{50} = 1.8, 13 and 106 μm, Table 1) and a rise of 7% in the porosity after sintering at 1500 °C was observed.

Although the porosity at 1500 °C increased, the total value is still rather low, indicating the high reactivity of the transition alumina generated. Therefore, it is reasonable to consider that replacing $Al(OH)_3$ by another hydrated compound, with greater mass loss and less sinterability, would result in higher porosity. An aluminum–magnesium double layered hydroxide, also known as hydrotalcite, was chosen for this purpose.

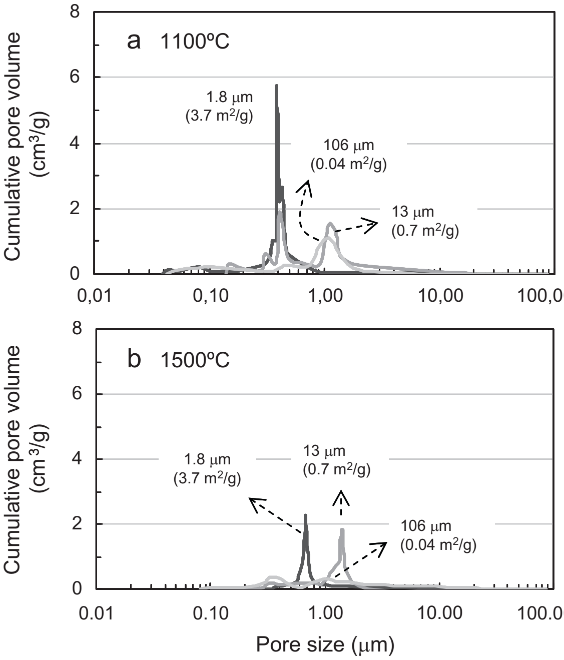

Fig. 3. Pore-size distribution for the samples prepared with different $Al(OH)_3$ particle size (and specific surface area) fired at (a) 1100 °C and (b) 1500 °C for 5 h.

3.3. Hydrotalcite as pore-former

Among the compounds with a composition favoring high refractoriness in the alumina–magnesia system and presenting significant amounts of hydroxyls and carbonates in their structures, those known as double-layer hydroxides (or hydrotalcite-like) [23–25] are good candidates to substitute $Al(OH)_3$. The general formula of the hydrotalcite-like compounds can be stated as $Mg_xAl_y(OH)_{2x+2y}(CO_3)_y\cdot 2(OH)_{16}\cdot nH_2O$, where $2 \leq x/y \leq 4$ [23], with a structure consisting of layers of ions of Mg^{2+} and Al^{3+} surrounded by atoms of oxygen, holding, among them, molecules of water and carbonate ions [25–27] (Fig. 4).

The hydrotalcites based on the reaction of MgO and hydratable alumina results in the $Mg_6Al_2CO_3(OH)_{16}\cdot 4H_2O$ compound [28,29]. It decomposes according to the following reaction:

$$Mg_6Al_2CO_3(OH)_{16}\cdot 4H_2O \rightarrow 6MgO + Al_2O_3 + 12H_2O + CO_2 \quad (3)$$

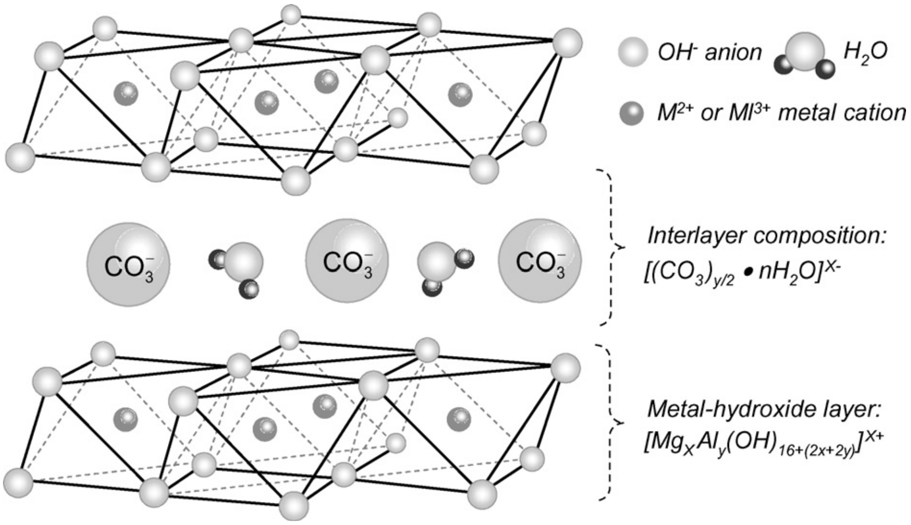

Fig. 4. Hydrotalcite's structure [26,28].

The total mass loss (as H_2O vapor and CO_2) for this compound is 43 wt.%, which is slightly higher to that shown by aluminum hydroxide (35 wt.%), and it decomposes at a similar temperature range (200–450 °C for hydrotalcite and 230–430 °C for $Al(OH)_3$) [23–25]. The resulting material comprises a mixture of 70 wt.% of magnesium oxide and 30 wt.% of aluminum oxide, both highly reactive. Besides acting as a pore-former, the reaction between MgO and Al_2O_3 leads to spinel ($MgAl_2O_4$) formation at temperatures above 1000 °C [30].

In order to analyze the use of the hydrotalcite as a pore-former, samples were prepared varying the content of hydrotalcite, in the alpha-alumina matrix, from 30 up to 97.5 wt.% (the 97.5 wt.% composition was comprised by hydrotalcite and CAC only). The resulting effects on porosity, mechanical strength and dimensional change are presented in Fig. 5. Samples containing $Al(OH)_3$ and hydrotalcite thermally treated at different temperatures can be seen in Fig. 6.

Firstly, it can be observed in Fig. 5a that porosity values significantly higher than those attained for the equivalent samples containing $Al(OH)_3$ were observed with the use of hydrotalcite for the 1500 °C thermal treatment temperature. This result could be initially associated to the difference of mass loss values between $Al(OH)_3$ and hydrotalcite (~8 wt.%) after decomposition. However, since differences of porosity greater than 20% were observed for these samples, it is reasonable to consider that it would be more likely related to the sintering-densification behavior of the whole system (pore former plus matrix). Secondly, the differences between the porosity values attained after thermal treatment at 1100 °C and 1500 °C were smaller for the hydrotalcite containing samples than the observed for those prepared with $Al(OH)_3$, which indicates lower densification at the higher temperature. Finally, the highest porosity levels were achieved for the samples containing 70 wt.% of hydrotalcite. The presence of maximum values of porosity and minimum ones for mechanical strength and shrinkage (Figs. 5b and c and 6) points out that the composition of the hydrotalcite–alumina system also plays an important role in this behavior. These hypotheses can be confirmed considering the results presented in Fig. 7 and previously published data reported in the literature [30–37].

The sample containing 70 wt.% hydrotalcite correspond to the 30 MgO:70 Al_2O_3 (w/w) ratio in the slurry (pore-former plus alumina–cement matrix). Fig. 7 shows that, after thermal treatment at 1500 °C, the components of these samples reacted generating spinel ($MgAl_2O_4$). No phases related to the presence of CAC (such as $CaO{\cdot}6Al_2O_3$ or $CaO{\cdot}MgO$, for example) were detected because the total amount of CaO in the system is below 1 wt.%. Spinel is well known for its sintering difficulty and when produced via solid state reaction of MgO and Al_2O_3 individual sources (such as $MgCO_3$ and $Al(OH)_3$ or, in the present case, mixing hydrotalcite and calcined alumina), its formation results in a 5 vol.% expansion and lower density which can result in microcracks in the surrounding structure [30–33]. Thus, during the decomposition of the precursors, a

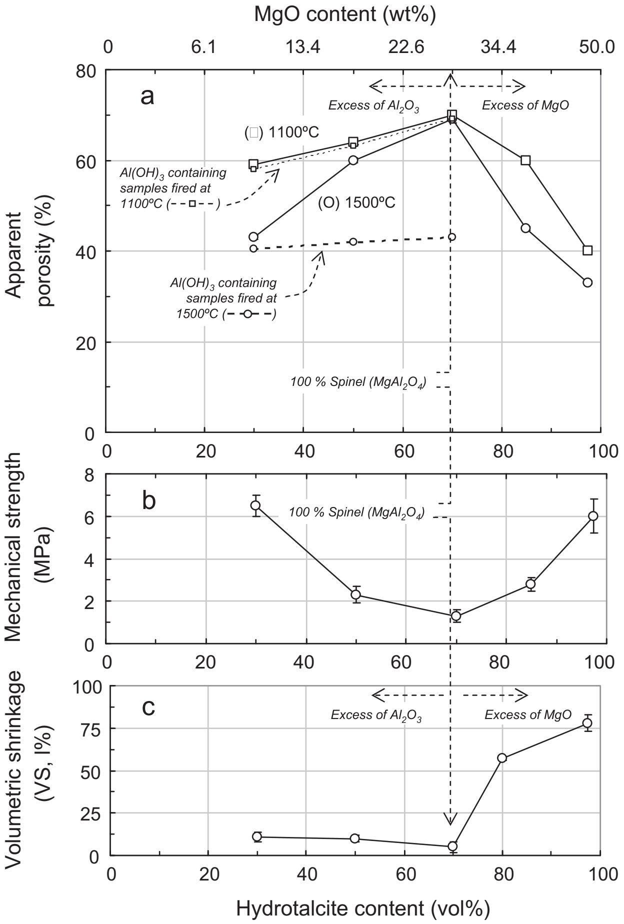

Fig. 5. (a) Apparent porosity, (b) mechanical strength and (c) volumetric shrinkage of samples prepared with different contents of hydrotalcite, fired at 1100 °C or 1500 °C for 5 h [the dotted lines show the results for the $Al(OH)_3$ containing samples].

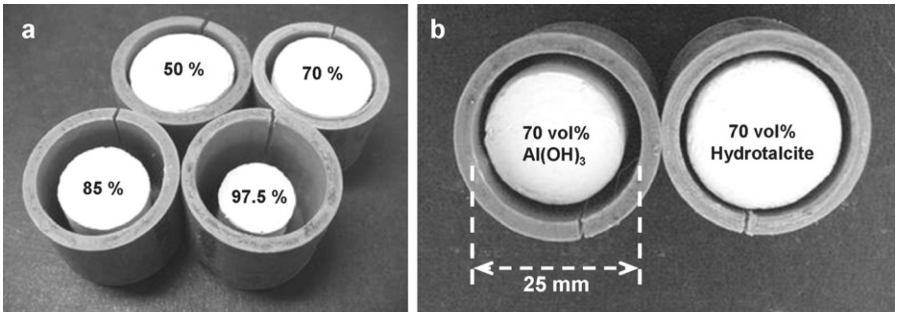

Fig. 6. Comparative view of the volumetric shrinkage for the samples prepared with (a) 50, 70, 85, and 97.5 vol.% of hydrotalcite and (b) 70 vol.% of different pore-formers, fired at 1500 °C for 5 h.

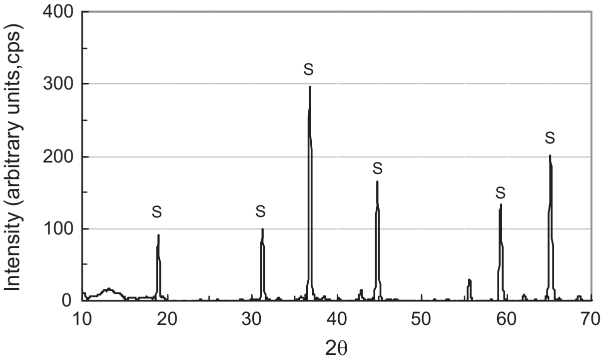

Fig. 7. X-ray diffraction pattern for the sample prepared with 70 vol.% of hydrotalcite (28 wt.% MgO and 72 wt.% Al_2O_3), fired at 1500 °C for 5 h, showing only spinel formation ($MgAl_2O_4$) (S).

great quantity of crystalline defects, pores and cracks are formed and must be rebuilt before sintering [30], usually causing abnormal grain growth and hindering its densification [35]. On the other hand, in systems where the stoichiometry of spinel is not attained (excess of Al_2O_3 or MgO), as in the present case for the samples with hydrotalcite contents lower or higher than 70 wt.%, greater densification is observed. This behavior can be explained considering the fact that for a certain temperatures ($\geq$1500 °C), spinel is a solid solution with a wide extent of composition. Due to this, Al_2O_3 or MgO can remain in the spinel lattice at temperatures above 1500 °C [30]. However, lowering the temperature of these systems, the solubility limits of these oxides in the spinel decreases and a second phase (corundum for Al_2O_3 or periclase for MgO) begins to precipitate at the grain boundaries, inhibiting grain growth and favoring densification [32,33]. Published results show that, for dense ceramics, the addition of 10 wt.% of MgO to spinel can lead to a decrease in the average grain size from 20 μm to 3 μm and an increase in the density from 3.41 g/cm^3 to 3.52 g/cm^3 [31–33].

The results attained in this paper by using hydrotalcite as a pore former, suggest that the sintering behavior of spinel ceramics, already known as a processing drawback for dense ceramics [32,37], regarding the generation of porous structures, can be very useful in preventing sintering at higher temperatures. Therefore, carefully tailoring the composition of the system, an optimal combination of (a) high porosity, (b) suitable mechanical strength and refractoriness, and (c) low volumetric shrinkage can be attained and preserved, even at a extended service life at high temperatures.

4. Remarks

Porous ceramics for applications such as thermal insulating can be produced by the decomposition of hydroxyl compounds such as $Al(OH)_3$ and/or hydro-carbonates (as hydrotalcite, $Mg_6Al_2(CO_3)(OH)_{16}\cdot 4H_2O$). The suitable choice of raw materials allowed for the generation of a great volume of pores during the decomposition of those compounds and sintering of the material. Samples prepared with $Al(OH)_3$ presented higher sensitivity to the temperature change and a significant reduction in porosity at temperatures above 1100 °C. This result was associated with the high reactivity of the transition alumina formed by $Al(OH)_3$ decomposition and the consequent densification of the alumina matrix. Those prepared with hydrotalcite, on the other hand, showed higher porosity even when fired at 1500 °C. This behavior was correlated to the presence of spinel which hindered densification and due to the expansive nature during its formation leading to microcrack generation.

Acknowledgements

The authors are grateful to the Brazilian Research Founding FAPESP and CNPq and Alcoa Aluminum (Brazil) for supporting this work and to Almatis (USA) and Magnesita S.A. (Brazil) for the raw materials supplied.

References

[1] V.R. Salvini, M.D.M. Innocentini, V.C. Pandolfelli, Optimizing permeability, mechanical strength of ceramic foams, American Ceramic Society Bulletin 79 (5) (2000) 49–63.

[2] A.R. Studart, U.T. Gonzenbach, E. Tervoot, L.J. Gauckler, Processing routes to macroporous ceramics: a review, Journal of the American Ceramic Society 89 (6) (2006) 1771–1789.

[3] O. Lyckfeldt, J.M.F. Ferreira, Processing of porous ceramics by starch consolidation, Journal of the European Ceramic Society 18 (2) (1998) 131–140.

[4] S. Dhara, P. Bhargava, A simple direct casting route to ceramic foams, Journal of the American Ceramic Society 86 (10) (2003) 1645–1650.

[5] F. Tang, H. Fudouzi, Y. Sakka, Fabrication of macroporous alumina with tailored porosity, Journal of the American Ceramic Society 86 (120) (2003) 2050–2054.

[6] I. Thijs, J. Luyten, M. Steven, Producing ceramic foams with hollow spheres, Journal of the American Ceramic Society 87 (1) (2003) 170–172.

[7] I. Garrn, C. Reetz, N. Brandes, L.W. Kroh, H. Shubert, Clot-forming: the use of proteins as binders for producing ceramic foams, Journal of the European Ceramic Society 24 (3) (2004) 579–587.

[8] M.O. Carlos, J.R. Garcia, I.R. Oliveira, R. Salomão, V.C. Pandolfelli, Porous ceramics through heterocoagulation process (in Portuguese), Cerâmica 318 (51) (2005) 78–84.

[9] P. Sepúlveda, F.S. Ortega, M.D.M. Innocentini, V.C. Pandolfelli, Properties of highly porous hydroxyapatite obtained by the gelcasting of foams, Journal of the American Ceramic Society 83 (12) (2000) 3021–3024.

[10] F.S. Ortega, P. Sepúlveda, V.C. Pandolfelli, Monomer systems for the gelcasting of foams, Journal of the European Ceramic Society 22 (9–10) (2002) 1395–1401.

[11] F.S. Ortega, F.A.O. Valenzuela, C.H. Scuracchio, V.C. Pandolfelli, Alternative gelling agents for the gelcasting of ceramic foams, Journal of the European Ceramic Society 23 (1) (2003) 75–80.

[12] V.R. Salvini, J.R. Garcia, I.R. Oliveria, V.C. Pandolfelli, Foaming agent and the effects on the physical properties of porous alumina (in Portuguese), Cerâmica 52 (321) (2006) 57–62.

[13] U.T. Gonzenbach, A.R. Studart, E. Tervoot, J.L. Gauckler, Macroporous ceramics from particle-stabilized wet foams, Journal of the American Ceramic Society 90 (1) (2007) 16–22.

[14] U.T. Gonzenback, A.R. Studart, D. Steinlin, E. Tervoot, J.L. Gauckler, Processing of particle-stabilized wet foams into porous ceramics, Journal of the American Ceramic Society 90 (11) (2007) 3407–3414.

[15] W. Mista, J. Wrzyszcz, Rehydration of transition aluminas obtained by flash calcination of gibbsite, Thermochimica Acta 331 (1) (1999) 67–72.

[16] Z. Deng, T. Fukasawa, M. Ando, High-surface-area alumina ceramics fabricated by the decomposition of $Al(OH)_3$, Journal of the American Ceramic Society 84 (3) (2001) 485–491.

[17] Z. Deng, T. Fukasawa, M. Ando, Microstructure and mechanical properties of porous alumina ceramics fabricated by the decomposition of hydroxide, Journal of the American Ceramic Society 84 (11) (2001) 2638–2644.

[18] P. Burtin, Influence of surface area and additives on the thermal stability of transition alumina catalyst supports. II: kinetic model and interpretation, Applied Catalysis 34 (1–2) (1987) 239–254.

[19] J. Zhao, M.P. Harmer, Effect of pore distribution on microstructure development: II first- and second-generation pores, Journal of the American Ceramic Society 71 (7) (1988) 530–539.

[20] R. Zhou, R.L. Snyder, Structures and transformation mechanisms of the η, γ and θ transition aluminas, Acta Crystallographyca B 47 (1991) 617–630.

[21] S. Kwon, G.L. Messing, Sintering of mixtures of seeded boehmite and ultrafine alpha-alumina, Journal of the American Ceramic Society 83 (1) (2000) 82–88.

[22] F.F. Lange, Sinterability of agglomerated powders, Journal of the American Ceramic Society 67 (2) (1984) 83–89.

[23] W.T. Reiche, Anionic clay minerals, Chemtech 1 (1986) 58–63.

[24] L. Pesic, S. Salipurovic, V. Markovic, D. Vucelic, W. Kagunya, W. Jones, Thermal characteristics of a synthetic hydrotalcite-like material, Journal Material Chemical 2 (10) (1992) 1069–1073.

[25] C.P. Kelkar, A.A. Schultz, L.A. Cullo, Synthesis of hydrotalcite-like materials with a sheet-like morphology, in: Synthesis of Porous Materials—Zeolites, Clays and Nanostructures, Marcel Dekker Inc., USA, 1997.

[26] A. Vaccari, Clay and catalysis: a promising future, Applied Clay Science 14 (4) (1999) 161–198.

[27] A. Vaccari, Layered double hydroxides: present and future, Applied Clay Science 22 (1–2) (2002) 75–76.

[28] K. Ghanbari, J.H. Sharp, W.E. Lee, Hydration of refractory oxides in castable bond systems-I: alumina, magnesia, and alumina–magnesia mixtures, Journal of the European Ceramic Society 22 (4) (2002) 495–503.

[29] G. Ye, T. Troczynski, Hydration of hydratable alumina in the presence of various forms of MgO, Ceramics International 32 (2006) 257–262.

[30] A.M. Alper, R.N. McNally, P.H. Ribbe, R.C. Doman, The system MgO–$MgAl_2O_4$, Journal of the American Ceramic Society 45 (6) (1962) 263–268.

[31] J.T. Bayley, R. Russel Jr., Sintered spinel ceramics, American Ceramic Society Bulletin 47 (11) (1968) 1025–1029.

[32] J.T. Bayley, R. Russel Jr., Preparation and properties of dense spinel ceramics in the $MgAl_2O_4$–Al_2O_3 system, Transactions of the British Ceramics Society 68 (4) (1969) 159–164.

[33] J.T. Bayley, R. Russel Jr., Magnesia-rich $MgAl_2O_4$ spinel ceramics, American Ceramic Society Bulletin 50 (5) (1971) 493–496.

[34] A.H. De Aza, P. Pena, M.A. Rodriguez, R. Torrecillas, S. De Aza, New spinel-containing refractory cements, Journal of the European Ceramic Society 23 (2003) 737–744.

[35] S.R. Shah, A.H. Chokshi, R. Raj, Porous Al_2O_3-spinel based polycrystals that resist free-sintering, Journal of the American Ceramic Society 91 (10) (2008) 3451–3454.

[36] M.A.L. Braulio, J.F.R. Castro, C. Pagliosa, L.R.M. Bittencourt, V.C. Pandolfelli, From macro to nanomagnesia: designing the in situ spinel expansion, Journal of the American Ceramic Society 91 (9) (2009) 3090–3093.

[37] I. Reimanis, H. Kleebe, A review on the sintering and microstructure development of transparent spinel ($MgAl_2O_4$), Journal of the American Ceramic Society 92 (7) (2009) 1472–1480.